STRUCTURAL AND THERMAL STUDY OF MESOMORPHIC DODECYLAMMONIUM CARRAGEENATES

M. Vinceković[1], A Pustak[2], Lj. Tušek-Božić[3], F. Liu[4], G. Ungar[4], M. Bujan[1], I. Šmit[2], N. Filipović-Vinceković[3]

[1]Department of Chemistry, Faculty of Agronomy, [2]Department of Materials Chemistry and [3]Department of Physical Chemistry, Ruđer Bošković Institute, Zagreb, Croatia
[4] Department of Engineering Materials, University of Sheffield, Sheffield, United Kingdom

Key words: dodecylammonium chloride, carrageenans, surfactant-polymer complexes

Address for correspondence.

Marko Vinceković, Ph. D.
Department of Chemistry
Faculty of Agriculture
Zagreb, Croatia
E-mail: mvincekovic@agr.hr

Abstract

Structural characteristics and thermal stability of a series of dodecylammonium carrageenates formed by stoichiometric complexation of dodecylammonium chloride and differently charged carrageenans (κ-, ι- and λ-carrageenan, respectively) were investigated. IR spectral analysis confirmed the electrostatic and hydrogen bond interactions between the dodecylammonium and carrageenan species. X-ray diffraction experiments show increased ordering in the complexes compared to that in the parent carrageenans. Dodecylammonium carrageenates have a layer structure, in which a polar sublayer contains layers of carrageenan chains and a nonpolar sublayer consists of conformationally disordered dodecylammonium chains electrostatically attached to the carrageenan backbone. The major factor that determines the dodecylammonium carrageenate structure is cationic surfactant, while the carrageenans moiety plays a major role in determining thermal properties.

1. Introduction

Surfactants and polymers play a major role in a variety of applications ranging from detergency, food processing, decontamination and purification, mineral processing, colloid stabilization to controlled release applications. Therefore, the study of interactions between surfactant and polymer is of interest for both science and practical applications. Extensive studies of the interactions in these mixtures have provided much insight into the phase behavior and structures formed. Self-organization was shown to occur from nano- to macroscopic length scale resulting in formation of various soluble and insoluble surfactant-polymer complexes (PSC) [1-10]. Substantial efforts have been made to clarify their structures, especially those in the solid state, because PSC represent a new and very interesting class of assembled materials [11]. In the solid state these complexes can exhibit mesophase characteristics of the bound surfactants, while the threading of polymer chains through the mesophase may create different geometrical constraints from small molecules, thus producing new structures. Numerous studies have demonstrated that the structure of the solid PSC can be tuned through variation in the charge density, flexibility, and hydrophobicity of the polymer chain as well as the surfactant properties, such as headgroup, alkyl tail, and polar-to nonpolar volume ratio [12-16].

In the last decades, complexes between biopolymers such as polysaccharides and oppositely charged surfactants have attracted a great interest in order to understand their functional role in formulated products such as food, cosmetics, pharmaceutics, thermoplastic materials, coating films, etc. These complexes are characterized by having

a very hydrophilic carbohydrate polymer associated with oppositely charged surfactants. The driving forces of complexation are the attractive electrostatic interactions between the charges and the hydrophobic interactions between the hydrocarbon chains of the surfactant.

Besides their widespread application in food industry, carrageenans have recently been used in some pharmaceutical formulations as a new and promising pelletisation aid in place of microcrystalline cellulose [17-19] as well as in synthesis of calcium phosphate nanocomposite scaffolds [20]. In this context it appears useful to investigate thermal stability of solid complexes of carrageenans with oppositely charged model amphiphilic compounds, a subject that had attracted only limited attention so far [21, 22].

This work is continuation of our systematic study of systems contaning differently charged carrageenans, *viz.* κ-, ι- and λ-carrageenan (denoted κC, ιC and λC, respectively), and the oppositely charged cationic surfactant dodecylammonium chloride (DDACl) [7, 8, 23]. Formation of various soluble complexes at the air/solution interface and in the bulk solution (from nano- to microdimensions), precipitation and gelation strongly depends on both, carrageenan and surfactant concentrations, their molar ratio and charge density on the carrageenan chains. Formation of giant vesicles even at low carrageenan concentrations [7, 8] and structural properties of collapsed gels [23] revealed lamellar ordering as an important feature of the dodecylammonium and carrageenan systems. In several papers Reynaers et al. [24-27] have shown that interaction of carrageenan gels with a cationic surfactant cetylpyridinium chloride (CPC) leads to the formation of a lamellar arrangement. Structural investigations of the carageenan and CPC at gelling conditions during reversible heating and cooling cycles have shown that no structural

transition are seen in the temperature range between the room temperature and 70 ^{o}C [25]. This means that addition of CPC stabilized the gel network structure in the temperature domain of the coil-helix transition. The present investigation was undertaken in order to explore structural and thermal properties of insoluble carrageenan/DDACl complexes precipitated from solutions where the carrageenan chains are present as random coils. It was shown that all complexes are less resistant to thermal degradation than the parent carrageenan compounds.

2. Experimental section

2.1 Materials and Sample Preparation

Carrageenans represent a well known polyelectrolyte series differing in the number and position of the sulphate groups: κC (ideally one sulphate group per monomeric unit), ιC (two), and λC (three). Scheme 1 shows the ideal structure of the disaccharide repeat units of all three carrageenans: κC (-(1→3)-β-D-galactopyranose-4-sulphate-(1→4)-3,6-anhydro-α-D-galactopyranose-(1→3)-), ιC (-(1-3)-β-D-galactopyranose-4-sulphate-(1-4)-3,6-anhydro-α-D-galactopyranose-2-sulphate-(1→3)-), and λC -(1→3)-β-D-galactopyranose-2-suphate-(1→4)-α-D-galactopyranose-2,6-disulphate-(1→3).

Commercial samples (Fluka, Germany) were purified by dialysis and subsequent percolation of respective aqueous solutions through an ion-exchange column with a cation exchange resin in the Na^{+}-form.

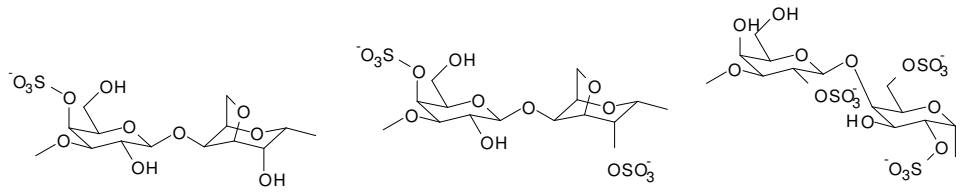

a b c

Scheme 1. Chemical structures of the ideal (a) κ-carrageenan (κC), ι-carrageenan (ιC), and λ-carrageenan (λC) repeat disaccharide units.

DDACl was used as model cationic surfactant for preparation of dodecylammonium carrageenate solid complexes (abbreviated $(DDA)_nCAR$). The preparation and purification of DDACl were described earlier [28]. Stock solutions were prepared by weight using redistilled water which was subsequently filtered through Millipore Type HA 0.10 μm to exclude dust before use.

Samples denoted with the common label $(DDA)_nCAR$ were prepared by mixing equivolume aqueous solutions of DDACl (0.1 mol/L) and one of the aforementioned carrageenan (1 % w/v) for 30 min at room temperature. The resulting individual dodecylammonium carrageenates are abbreviated DDAκC, $(DDA)_2ιC$, $(DDA)_3λC$, respectively. The precipitate was collected by filtration and eventually the coprecipitated NaCl was washed away with cold water. All $(DDA)_nCAR$ were dried in vacuum at room temperature.

Elemental analysis of the precipitates confirmed the formation of nearly stoichiometric solid complexes in terms of charge per disaccharide unit, according to the relation

$$nDDA^+ + (CAR)^{-n} \rightarrow (DDA)_nCAR,$$

where n is 1, 2 or 3 for κC, ιC and λC, respectively.

2.2. Methods

FTIR spectra from KBr pellets were recorded in the 4000-250 cm^{-1} region on an ABB Bomen MB102 spectrometer at a resolution of 4 cm^{-1}.

Differential thermogravimetry (DTG) was done on a Mettler TA 4000 System, and differential scanning calorimetry (DSC) on TA Instruments, Model DSC 2910 calorimeter at a 5 $^{o}C\ min^{-1}$ heating rate. All results were taken from the first heating run. The transition temperatures were reported as the minima and maxima of their endothermic and exothermic peaks. The data presented are mean values of several independent measurements on different samples, the standard deviation being of the order of ±5 K.

The morphology and texture of solid phases were observed by a polarizing light microscope (Leica DM LS) equipped with a Mettler FP 82 hot stage and a camera.

X-ray powder diffraction (WAXD) was performed with a Philips 1050 diffractometer (with monochromatic CuK_{α} radiation and a proportional counter) at room temperature (RT). The overall diffraction angle region was $2\theta^{o}$ = 1.5-50^{o}. WAXD patterns at lower diffraction angles $2\theta^{o}$ = 1.5-5^{o} were obtained with appropriate slit collimation.

Small-angle X-ray diffraction measurements (SAXS) were carried out on station I22 at the Diamond Light Source in the Bragg´s angle region 2θ = 0.1 – 2.5. Samples were held in 1 mm capillaries with 10 μm walls, placed in a modified Linkam hot stage with mica windows. A Rapid II (Daresbury Detector Group) multiwire area detector was used, and

XFIX (CCP13) was used for radial intensity scans. In-house software was used for further processing.

3. Results and Discussion

3.1. Structural characterization

3.1.1. Evidence of complexation

Infrared investigations on dodecylammonium carrageenates showed that their spectra were not simple superpositions of the corresponding spectra of parent components. The vibration bands of the ammonium and sulphate groups of the complexes were compared to those of the parent components ((for example see Fig. 1 for DDACl, ιC and $(DDA)_2$ιC).

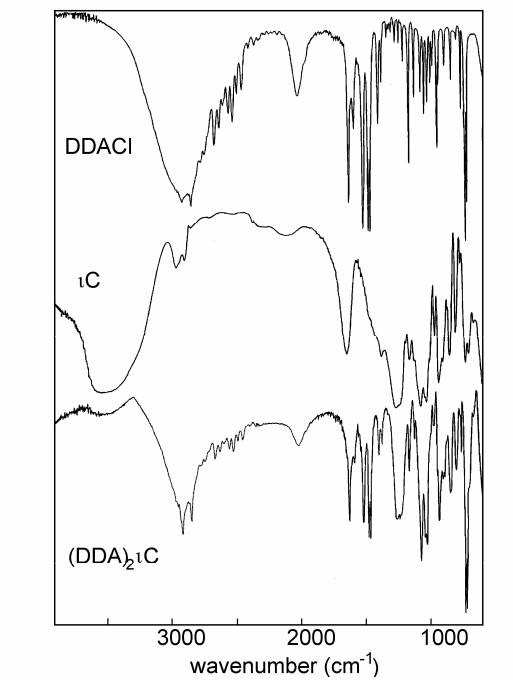

Fig.1. FTIR spectra of DDACl, ιC and $(DDA)_2$ιC.

A strong and very broad NH_3^+ stretching absorption around 3000 cm^{-1} detected in DDACl is greatly reduced in intensity in $(DDA)_n$CAR. Overlapping at the low frequency side are the alkane CH stretching absorptions appearing as two bands at 2915 and 2851 cm^{-1}. In addition, a complex absorptions bands covering the region from 2700 to 2400 cm^{-1}, as well as a band around 2020 cm^{-1} ascribed to overtones and combinations [29] were found to be less intense in $(DDA)_n$CAR than in DDACl, while the NH_3^+ bending band at 1518 cm^{-1} is shifted towards lower frequencies by 5 cm^{-1}. Spectral changes may be noticed also in the sulphate absorptions between 1280 and 800 cm^{-1}. All parent carrageenans show the characteristic intense and broad absorption around 1250 cm^{-1} (appearing in κC and ιC as a doublet with maxima of nearly equal intensity at about 1270 and 1230 cm^{-1}). This absorption corresponds to the asymmetric stretching of ester sulphate O=S=O groups. Its intensity decreased from λC to ιC and κC, which is in accordance with the number of substitutions by sulphate groups [30]. In $(DDA)_n$CAR these bands are shifted to lower wave numbers by 10-15 cm^{-1}. The symmetric sulphate stretching vibration is superimposed upon the more intense C-O and C-OH absorptions characteristic of all polysaccharides, which occurred between 1080 and 1040 cm^{-1}. The intense band at 1029 cm^{-1} arising from the pseudo-symmetric O=S=O stretching in C-2 of 3,6-anhydrogalactose is present in ιC and λC, that in C-6 appears only in λC at 1012 cm^{-1}. However the position of such a vibration is difficult to attribute unequivocally to the sulphate on C-4 of the galactose due to the overlap with other bands. The C-O-S stretching bands could be used to determine the sulphate position precisely. Thus the band at 848 cm^{-1} due to sulphate on C-4 of the galactose shows up in κC and ιC [31], the band at 805 cm^{-1} associated with the axial secondary sulphate on C-2 of the 3,6-

anhydrogalactose appears only in ιC [32], while the stretching C-O-S band of the equatorial secondary sulphate on C-2 and C-6 of galactose at 835 cm^{-1} is present only in λC [33].

Upon carrageenan complexation most sulphate bands are shifted slightly (up to 8 cm^{-1}) to lower frequencies. The presence of water in carrageenans, detected by TGA (see below) is confirmed by strong and very broad absorption centred between 3500-3400 cm^{-1}, overlapping the carrageenan OH stretching vibrations. The OH bending absorption appears as a medium to strong band at about 1650 cm^{-1}. In the carrageenate complexes the OH stretching band is also broad but weak, while the OH bending band is shifted to lower frequencies by 20 cm^{-1}. This spectral pattern is consistent with the polysaccharide hydroxyl groups in $(DDA)_nCAR$ being involved in hydrogen bonding.

In conclusion, comparison of the IR spectra confirmed complex formation due to the electrostatic interactions between the dodecylammonium and carrageenan ionic species and hydrogen bonding of polysaccharide hydroxyl groups.

3.1.2. X-ray diffraction analysis

Powder X-ray diffractograms of parent carrageenans showed only diffuse scattering (not shown) indicating that the material was amorphous. On the other hand, it has been reported that in polycrystalline and oriented κC and ιC fibers carrageenan chains form double stranded helices arranged laterally in a trigonal unit stabilized by SO_3^--Na-SO_3^- interactions [34-37]. Unlike κC and ιC, the structure of the non-gelling λC is poorly documented.

Fig. 2 shows diffractograms of dodecylammonium carrageenates (curves a, b, c) and DDACl (curve d). DDACl crystallizes from solution showing diffractogram with a number of sharp diffraction lines in the wide angle region. The 1:2 ratio of reciprocal spacings for the first two reflections at smaller angles suggests lamellar ordering. Furthermore, the strongest diffraction lines in the wider angle region of the DDACl were identified as multiple orders of diffraction from (00*l*) crystal planes. The lamellar thickness is determined as 1.79 nm, which corresponds to interdigitated layer [38-40].

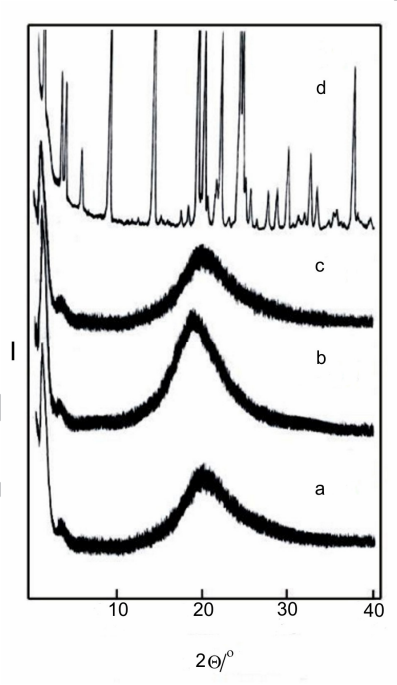

Figure 2. WAXD diffractograms of (a) DDAκC, (b) $(DDA)_2$ιC, (c) $(DDA)_3$λC and (d) DDACl.

All $(DDA)_n$CAR diffractograms display two reflections in the small angle region and one pronounced diffuse diffraction maximum in a wider-angle region. The diffraction halo at 2Θ ~ 20˚, typical for disordered liquid-like conformation of liquid paraffins [41], suggests short-range order of hydrocarbon chains in lamellae. DDACl induced the

formation of mesostructures in carrageenans, *i*.e. the carrageenan chains fill the space between the dodecylammonium lamellae (with NH_3^+ head groups electrostatically bound to sulfate groups). The induced ordering is the result of electrostatic and hydrophobic interactions as well as of hydrogen bonding. The thickness of lamellae corresponding to the interplanar spacing (d_{001}) calculated from the first diffraction maximum is d_{001} = 3.84 nm for DDAκC, d_{001} = 3.46 nm for $(DDA)_2$ιC, and d_{001} = 3.60 nm for $(DDA)_3$λC. Considering that fully extended length of the dodecyl chain (1.67 nm [42]), ionic radii of ammonium and sulphate groups (0.25 nm and 0.40 nm) [43] as well as the outer radius of polysaccharide backbone (~ 0.75 – 1.00 nm) [37], calculated thickness of lamellar layer (~ 3.07 to 3.32 nm) is lower than experimentally determined interplanar spacing values. This difference may arise by filling of intralamellar space with of disordered hydrocarbon chains with irregular conformation with respect to the carrageenan backbone. It is therefore apparent that the interactions between carrageenan chains and surfactant result in the formation of a layered structure of the surfactant with irregular conformations in conjunction with the carrageenan chains. That is, the structure of the solid complexes consists of two domains: one nonpolar composed of alkyl chains and the other polar composed of carrageenan backbones.

The most intensive first maximum and amorphous halo of $(DDA)_2$ιC indicates enhanced lamellar stacking in $(DDA)_2$ιC system [7] and can be explained with two sulphate groups located on the both side of polysaccharide backbones with symmetrically bonded paraffin chains. Location of one or three sulphate groups in κC and λC backbones induced asymmetric binding of alkyl chains to one or three sulphate groups and greater disordering inside lamellae. WAXD patterns of all $(DDA)_n$CAR with the 1:2

relationship of the reciprocal interplanar spacing of two small-angle maxima indicated their lamellar ordering. Similar second order diffraction maximum, suggesting lamellar type of ordering, has been also observed in the small-angle X-ray scattering (SAXS) patterns of κC and ιC complexes with cationic surfactants [23-27].

3.2. Thermal behavior

3.2.1. Water loss and degradation

A comparison of weight loss (TGA) and derivative of weight loss (DTG) curves of $(DDA)_nCAR$ with those of the parent compounds could be seen in Fig. 3. From DTG curves, the temperature of maximum weight loss was determined. DDACl showed no presence of moisture. The mass loss of DDACl occurred in two stages with maxima at 287 ^oC and 317 ^oC (Fig. 3(a)). The main products of decomposition are $C_{12}H_{25}NH_2$ and HCl in gaseous state [44].

The parent carrageenans showed complex behavior of mass loss (Figures. 3(b)-(d)). Carrageenan samples dehydrated slowly in a broad temperature range up to ~ 140 ^oC. κC, ιC and λC lost, respectively, 13.6, 15.8 and 12.5 % of mass in total. The mass loss corresponding to moisture was much smaller for $(DDA)_nCAR$ (4.3, 3.9 and 3.6 % for DDAκC, $(DDA)_2$ιC and $(DDA)_3$λC, respectively). At higher temperatures both $(DDA)_nCAR$ and the parent carrageenans DTG curves exhibited two to three peaks indicating mass loss in several steps.

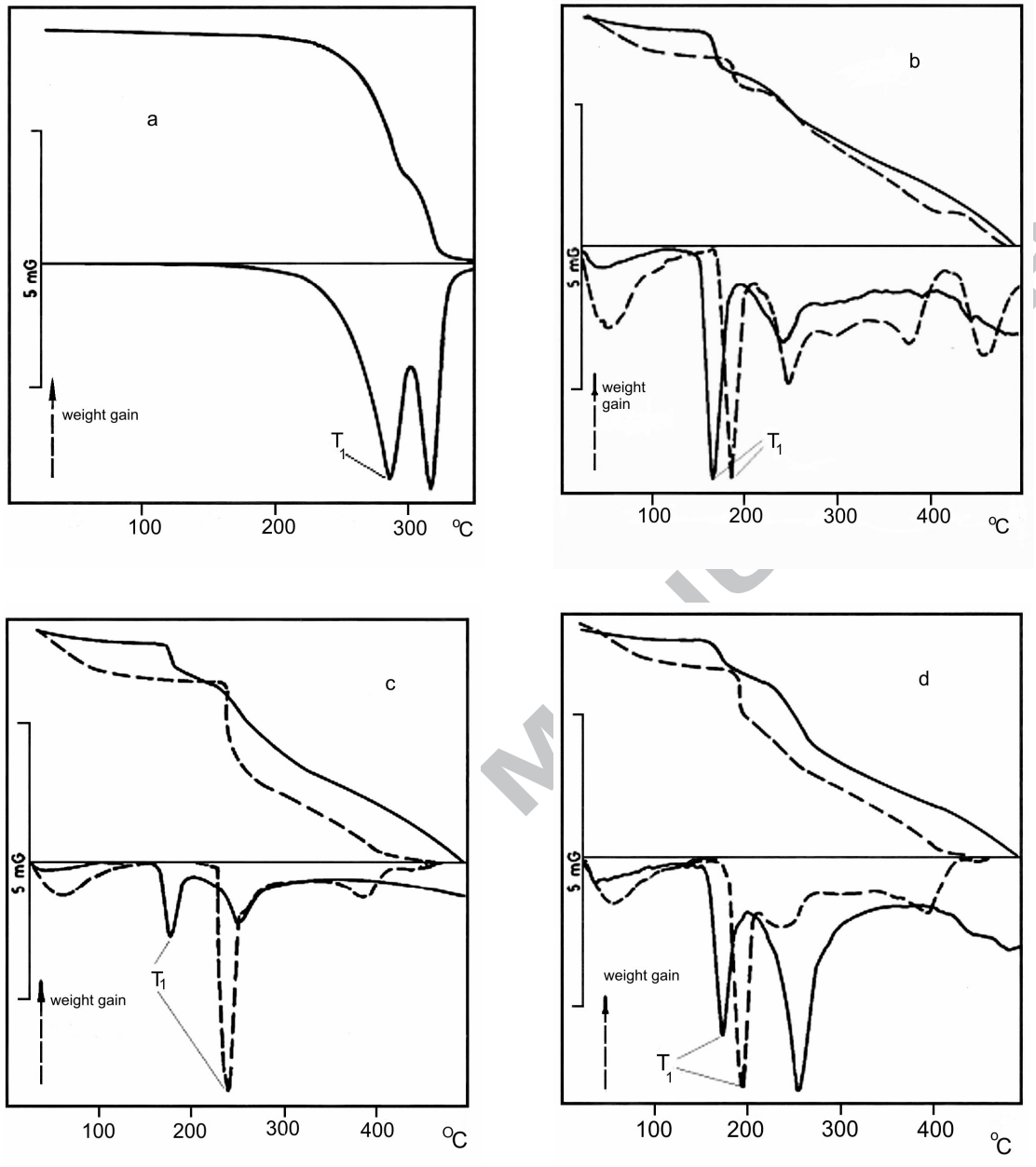

Figure 3. TGA (top) and DTG (bottom) curves of (a) DDACl, (b) κC (dashed line) and DDAκC (full line), (c) ιC (dashed line) and $(DDA)_2$ιC (full line), and (d) λC (dashed line) and $(DDA)_3$λC (full line).

Table 1.
Thermal degradation data of dodecylammonium carrageenates $(DDA)_nCAR$ and parent compounds; dodecylammonium chloride (DDACl), κ-, ι- and λ- carrageenan (κC, ιC, λC). T is maximum decomposition temperature for the main steps and w is corresponding mass loss.

COMPOUND	T_1/°C	w_1/%	T_2/°C	w_2/%	T_3/°C	w_3/%
DDAκC	165.0	17.06	242.0	30.28		
κC	183.7	11.97	246.7	34.00	374.0	11.07
$(DDA)_2$ιC	176.7	16.95	251.0	24.89		
ιC			235.0	43.05	382.0	16.78
$(DDA)_3$λC	174.8	16.02	256.0	44.70		
λC	193.0	45.03	241.0	12.50	394.0	14.00
DDACl	286.7	60.00	316.7	31.34		

Thermal degradation data of $(DDA)_nCAR$ and their parent compounds are illustrated in Table 1. Data for moisture loss are not shown. The first sharp peak in DTA curve (denoted as T_1) indicated partial degradation of both, $(DDA)_nCAR$ and parent carrageenans. The degradation of carrageenans was investigated by a combination thermogravimetric analysis and mass spectroscopy [18]. It was shown that the degradation is associated with carbon dioxide and sulfur dioxide leaving and carbohydrate backbone fragmentation. After moderately fast degradation there was almost steady slow decomposition up to 500 °C occurring in several steps.

Complexation of carrageenans with DDACl affected their thermal behavior. Generally, all $(DDA)_nCAR$ were less thermally stable, *i.e.* the maximum temperature of the first step in decomposition was somewhat lower compared to that of the corresponding parent carrageenans.

3.2.2. DSC analysis

Figures 4 and 5 present a set of DSC heating curves for parent compounds and their complexes with DDACl.

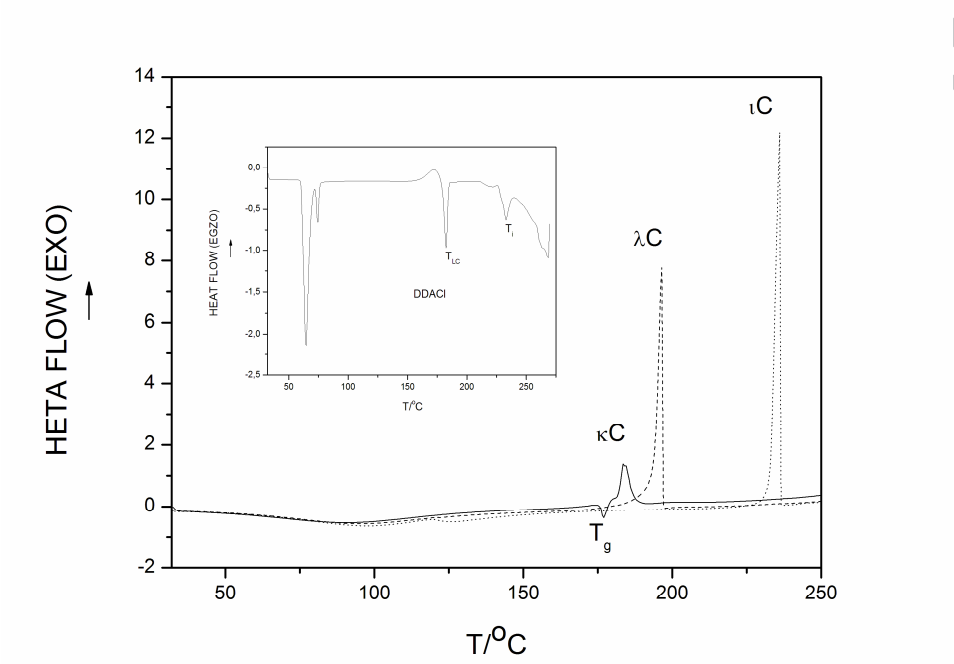

Fig. 4. DSC curves of the parent carrageenans (κC, ιC and λC) and DDACl (inset: T_{LC} is liquid crystallization temperature, T_i is isotropization temperature) on the first heating scan. κC – solid line; ιC –dashed line; λC – dotted line; T_g is glass transition temperature.

DDACl heating scan (inset in Fig. 4) shows a complex sequence of endothermic transitions (i.e. several polymorphic transitions in the crystalline phase, transition from crystal (K) to liquid crystal (LC) and further to the isotropic liquid (IL). Microscopic observation under crossed polarizers showed oil streak textures indicating the formation of a smectic A phase which exists up to isotropic liquid. Beyond the exothermic formation of the LC phase, no further transition was observed by DSC until decomposition. The cooling DSC scan of DDACl shows hysteresis (not shown). X-ray analysis had shown that the transitions during heating involve a change from a room

temperature monoclinic structure to a high temperature tetragonal form, while the LC phase is smectic A in nature. On subsequent cooling the crystals return to a secondary monoclinic structure [38-40].

A common feature of heating curves of the carrageenans is the presence of broad endothermic transitions at lower temperature corresponding to the moisture loss. DSC scan for the pure κC shows the second endothermic peak closely spaced to the sharp exothermic peak. This endothermic peak may be ascribed to the glass transition. Sharp exothermic peaks observed for all parent carrageenans are associated with partial degradation.

DSC scans for $(DDA)_nCAR$ are presented in Fig. 5. Similarly to the parent carrageenans, all complexes show one broad endothermic transition at lower temperature corresponding to the moisture loss and a sharp exothermic transition at higher temperatures corresponding to partial decomposition. Only in DDAκC scan the glass transition was detected approximately at the same temperature like in parent κC. It suggests the glass transition of rigid carrageenan macromolecules in DDAκC as well as in κC. This transition occurs in DDAκC immediately after partial fragmentation of carrageenan chains. Significantly smaller enthalpy change (Table 2) at glass transition of DDAκC indicates partial fragmentation enhances flexibility of rigid carrageenan macromolecules thus alleviating glass transition.

Observation under polarization microscope have shown that at the exothermic transitions of the parent carrageenans and their complexes with DDACl the sample surface appeared black and all heated samples displayed only small birefringence under crossed polarizers without expressed textures.

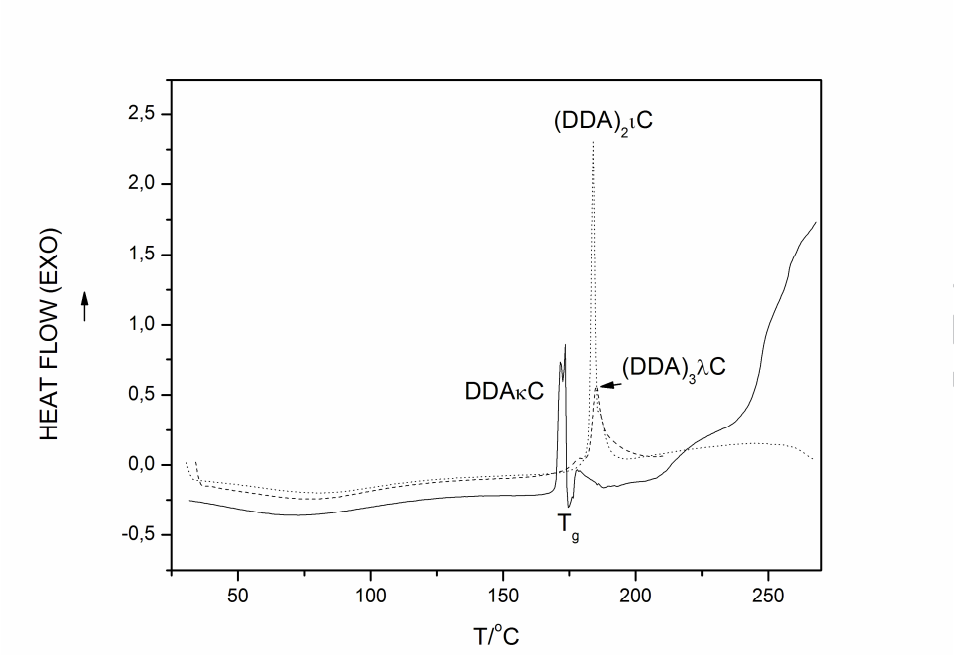

Fig. 5. First heating DSC curves of $(DDA)_nCAR$. DDAκC – dotted line; $(DDA)_2$ιC – solid line; $(DDA)_3$ λC – dashed line. T_g – glass transition temperature.

Table 2.
Peak transition temperature (T) and molar enthalpy change (ΔH) for κC, ιC , λC, $(DDA)_x$CAR and DDACl in the first heating cycle.

COMPOUND	**T/**°C	**ΔH/**kJ mol^{-1}	**T/**°C	**ΔH/**kJ mol^{-1}	**T/**°C	**ΔH/**kJ mol^{-1}
κC	93	120.2	177	5.7	183	- 20.2
ιC	99	208.1			236	- 98.6
λC	95	185.6			196	- 133.9
DDAκC	72	67.1	176	0.59	172	- 22.2
$(DDA)_2$ιC	82	52.4			184	- 59.3
$(DDA)_3$λC	79	75.6			185	- 61.4
DDACl	64	25.5	182	8.9	233	5.0

Peak transition temperatures and corresponding molar enthalpy changes for parent compounds and their complexes are listed in Table 2. The absolute value of molar enthalpy change associated with the exothermic transition with increasing number of

sulphate groups exhibited higher increase for the parent carrageenans than their corresponding complexes.

3.2.3. SAXS analysis

At room temperature the structure of the $(DDA)_nCAR$ mesophase is envisaged as consisting of carrageenan chains entrapped between dodecylammonium lamellae with NH_3^+ head groups electrostatically bound to the sulphate groups on the backbone. The induced ordering in comparison with parent carrageenans is the result of a combination of electrostatic and hydrophobic interactions as well as of hydrogen bonding.

The pronounced glass transitions observed in both κC and corresponding complex with DDACl indicated that structural ordering of DDAκC during heating should be expected. SAXS curves were recorded as a function of temperature. In order to minimize the exposure of the samples to high temperatures and avoid further degradation, recordings on heating were not made above 170 °C. Figure 6 presents the Lorentz-corrected SAXS intensity curves $Iq^2(q)$ versus the scattering vector q [$\boldsymbol{q} = (4\pi/\lambda) \sin\theta$, with λ the X-ray wavelength]. Where Bragg reflections were observed, their spacings are listed in Table 3. In all cases but one the reflections are the 1st and 2nd orders of the fundamental layer diffraction from the lamellar LC (smectic) phase.

At room temperature (DDA)κC displays a diffuse low-angle peak centered at $q = 1.6$ nm^{-1}, indicating the absence of long range positional order, but rather the presence of short-range smectic-like fluctuations, typical of the isotropic phase of amphiphiles (Fig. 6). Glassy state is considered responsible for the failure to form periodic packing [41].

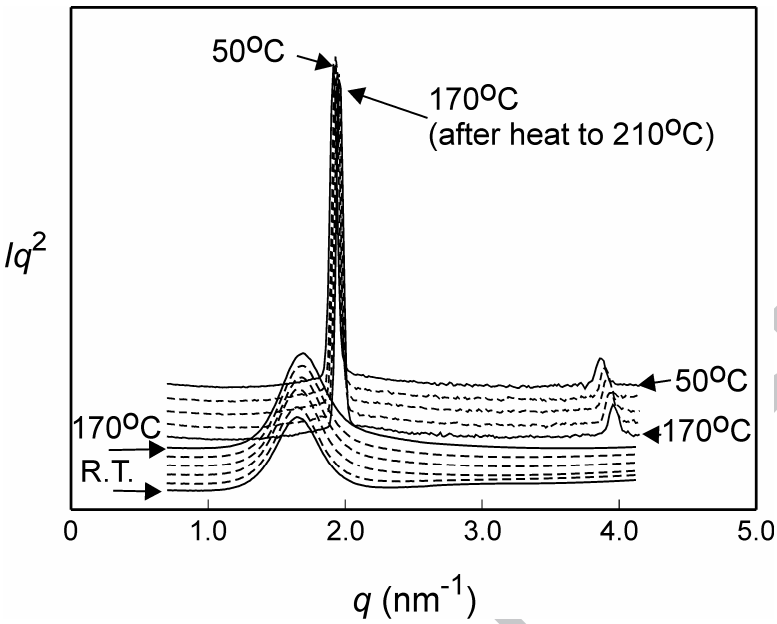

Fig. 6. Temperature dependence of SAXS patterns of DDAκC during heating from R.T. to 170 °C (bottom half) and during cooling from 170 °C to 50 °C (top half). Between the heating and cooling ramps, the sample was briefly heated to 210 °C. The successive curves are shifted vertically for clarity.

Heating of (DDA)κC up to 170 °C causes only a marginal shift of the diffuse maximum, with no indication of any significant restructuring. After heating to 210 °C this maximum sharpens and shifts to ~ 2.0 nm^{-1}, concomitant with the appearance of the sharp second diffraction order. This is consistent with ordering process and the formation of the layered mesophase. The moderate increase in lamellar spacing on lowering the temperature is consistent with the gradual extension and decreasing conformational disorder of the alkyl chains in the aliphatic sublayer.

A comparison of molecular mass of repeated unit with carrageenan chain (408 vs. 327000 Da, [45]), may indicate that partial degradation causing fragmentation of carrageenan macromolecules does not significantly change layered domain ordering of carrageenan chains. It seems that change in *d*-spacing is mainly associated with structural ordering in

nonpolar domain containing alkyl chains, i.e. the relaxed carrageenan macromolecules with enhanced flexibility enable better ordering of alkyl chains inside layers.

Table 3
d-spacings corresponding to the first and second-order layer reflections of DDAκC complex as a function of temperature; R.T. denotes the room temperature.

Temperature (^{o}C)	*d*-spacing(nm)
Heating	
R. T.	3.84
50	3.85
80	3.84
110	3.83
140	3.82
170	3.81
Cooling after short annealing at 210 ^{o}C	
170	3.17
	1.16
140	3.19
	1.59
110	3.18
	1.60
80	3.22
	1.60
50	3.25
	1.62

Different models were built, with the constraints of the experimentally observed layer periodicity and an assumed density of 1 g cm^{-3}. The modeling was performed with the sole purpose of comparing the viability of different models with respect to such criteria as

space filling and approximate layer thickness. After energy minimization, the models were subjected to a short annealing NVT molecular dynamics simulation (Forcite Plus module and the Universal Force Field, Material Studio, Accelrys; rhombic prism box with periodic boundary conditions; height equal to experimental layer spacing, thickness 0.45 nm).

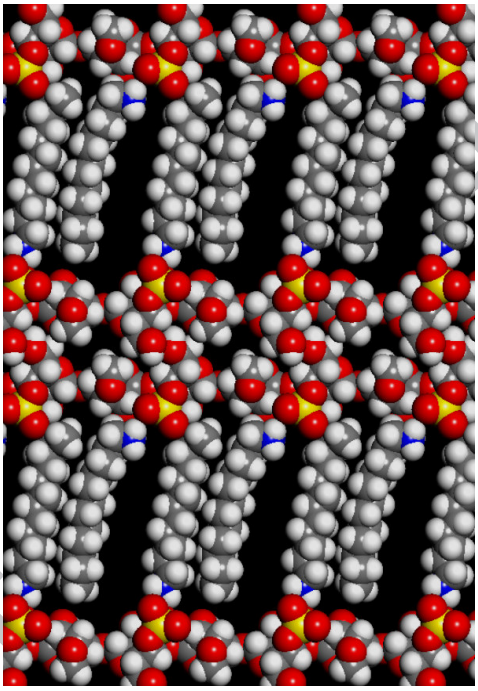

Fig. 7. Model of DDAκC in the layered LC state after a short annealing dynamics simulation: carbon (dark gray), hydrogen (light gray), oxygen (red), sulphate (yellow), nitrogen (blue).

Figure 7 shows the molecular organization of DDAκC after the annealing. The layers consist of a polar sublayer containing the carrageenan and the ammonium groups, while the nonpolar sublayer contains the fully interdigitated dodecyl chains. On average, each

polar sublayer contains two carrageenan chains in thickness. As the alkyl chains are fully interdigitated, the structure can be described as a monolayer rather than a bilayer.

A similar structure is also exhibited by $(DDA)_2\iota C$ and $(DDA)_3\lambda C$ as well as smectic and crystalline polymer electrolytes [46]. In the latter case the alkyl chains are covalently bonded to the modified poly(ethylene oxide) backbone.

4. Conclusions

Interactions between hydrophilic carrageenan biopolymers and the oppositely charged DDACl cationic surfactant result in the formation of insoluble stoichiometric complexes. As-precipitated and dried, all complexes were in mesomorphous state. On heating the complexes undergo a remarkably sharp exothermic transformation into a lamellar liquid crystal phase in which the polar sublayer contains ammonium groups attached to the carrageenan chains arranged in rafts, two chains in thickness; at the same time the nonpolar sublayer contains the fully interdigitated alkyl chains. The sharp exothermic transitions of complexes are comparable to those in free carrageenans but occur at lower temperatures and have a smaller change in molar enthalpy. Complexation of carrageenans with DDACl affects their thermal stability; all $(DDA)_n$CAR are less resistant to thermal degradation, *i.e.* the onset decomposition temperature is lower than that of the parent carrageenan compounds. The major factor determining the type of $(DDA)_n$CAR structure is DDACl, while the carrageenan chains act as a binder holding together the charged surfactant head groups. The absence of wide-angle Bragg reflections proved that no surplus crystalline DDACl remained after

complexation.

Acknowledgements

We thank Dr. Nick Terrill for assistance with setting up the SAXS experiment and Diamond Light Source for the beam time on I22. We are also grateful to Dr. Xiangbing Zeng for carrying out the SAXS experiment.

References

1. L. Picullel, B. Lindman, Adv. Colloid Interface Sci. 11 (1992) 149.
2. M. Goldraich, J. R. Schwartz, J. L. Burns, Y. Talmon, Colloids Surf. A: Physicochem. Eng. Asp. 125 (1997) 231.
3. I. Iliopoulos, Curr. Opin. Colloid Interface Sci. 3 (1998) 493.
4. B. Jönson, B. Lindman, K. Holmberg, K. Kronberg, Surfactant and Polymers in Aqueous Solution, John Wiley & Sons Ltd., Chichester, 1998.
5. J. C. T. Kwak, Polymer-Surfactant Systems, Surfactant Science Series 77, Marcel Dekker, New York, 1998,
6. P. Hansson, Langmuir 17 (2001) 4167.
7. M. Vinceković, M. Bujan, I. Šmit, N. Filipović-Vinceković, Colloids Surf. A: Physicochem. Eng. Asp. 255 (2005) 181.
8. V. Tomašić, A. Tomašić, N. Filipović-Vinceković, J. Colloid Interface Sci. 256 (2002) 462.
9. N. Caram-Lelham, F. Hed, L. O. Sundelöff, L. O. Biopolymers 41 (1997) 765.
10. B. Persson, N. Caram-Lelham, L. Sundelöff, L. O. Langmuir 16 (2000) 313.
11. S. Zhou and B. Chu, Adv. Mater. 12 (2000) 545.
12. M. Antonietti, A. Kaul, A. Thünemann, Langmuir 11 (1995) 2633.
13. M. Antonietti, M. Maskos, Macromolecules 29 (1996) 4199.
14. M. Antonietti, D. Radloff, U. Wiesner, H. W. Spiess, Macromol. Chem. Phys. 197 (1996) 2713.
15. K. Kogej, E. Theunissen, H. Reynaers, Langmuir 18 (2002) 8799.

16. A. F. Thünemann, Progr. Polym. Sci. 27 (2002) 1473.

17. M. Thommes, P. Kleinebudde, Europ. J. Phar. Sci. 63 (2006) 59.

18. M. Thommes, W. Blaschek, P. Kleinebudde, Europ. J. Pharm. Sci. 31 (2007) 112.

19. M. C. Bonferoni, S. Rossi, F. Ferrari, G. P. Bettinetti, C. Caramella, Int. J. Pharm. 200 (2000) 207.

20. A. L. Daniel-da Silva, A. B. Lopes, J. Mater. Sci. 42 (2007) 8851-8591.

21. C. Lii, H. Chen, S. Lu, P. Tomasik, Int. J. Food Sci. Techn. 38 (2003) 787.

22. C. Lii, H. Chen, S. Lu, P. Tomasik, J. Polym. Environ. 11 (2003) 115.

23. M. Vinceković, M. Bujan, I. Šmit, Lj. Tušek-Božić, D. Tsiourvas, M. Dutour Sikirić, J. Disper. Sci. Techn. 29 (2008) 966.

24. E. V. Shtykova, E. V. Jr. Shtykova, V. Volkov, A. T. Konarev, A. Dembo, E. Makhaeva, I. A. Ronova, A. Khokhlov, H. Reynaers, D. I. Svergun, J. Appl. Cryst. 36 (2003) 669.

25. G. Evmenenko, E. Theunissen, H. Reynaers, J. Polym. Sci., Polym. Phys. 38 (2000) 2851.

26. G. Evmenenko, E. Theunissen, K. Mortensen, H. Reynaers, Polymer 42 (2000) 2907.

27. K. Kogej, G. Evmenenko, E. Theunissen, J. Škerjanc, H. Berghmans, H. Reynaers, W. Bras, Macromol. Rapid Comm. 21 (2000) 1226.

28. N. Filipović-Vinceković, M. Bujan, N. Nekić, Đ. Dragčević, Colloid Polym. Sci. 273 (1995) 182.

29. R. M. Silverstein, F. X. Webster, Spectrometric Identification of Organic Compounds, 6th Edition, Wiley, New York, 1998.

30. J. Prado-Fernandez, J. A. Rodrigues-Vazquez, E. Tojo, J. M. Andrade, Anal Chim. Acta 480 (2003) 23.

31. M. Sekkal, P. Legrand, Spectrochim. Acta 49A (1993) 209.

32. M. Sekkal, P. Legrand, J. P. Huvenne, M. C. Verdus, J. Mol. Struct. 294 (1993) 227.

33. T. Chopin, E. Whalen, Carbohydr. Res. 246 (1993) 51.

34. S. Arnott, W. E. Scott, D. A. Rees, C. G. A. McNab, J. Mol. Biol. 90 (1974) 253.

35. N. S. Anderson, J. W. Campbell, M. M. Harding, D. A. Rees, J. W. B. Samuel, J. Mol Biol. 45 (1969) 85-99.

36. R. P. Millane, R. Chandrasekaran, S. Arnott, I. C. M. Dea, Carbohyd. Res. 182 (1988) 1.

37. S. Janaswamy, R. Chandrasekaran, Carbohyd. Res. 335 (2001) 181-194.

38. A. Terreros, P. A. Galera Gomez, E. Lopez Cabacros, J. Therm. Anal. Calorimetry 61 (2000) 341.

39. D. F. R. Gilson, A.S. Kertes, R. St. J. Manley, J. Tsau, Can. J. Chem. 54 (1976) 765.

40. G. J. Kruger, D. G. Billing, M. Rademeyer, in: J. C. A. Boeyens, J. F. Ogilvie (Eds.). Models, Mysteries and Magic of Molecules, Springer, Darmstadt, 2008, p. 219.

41. V. Luzzati, in: D. Chapman (Ed.) Biological Membranes. Physical Fact and Function, Academic Press, London and New York, 1968, p. 71.

42. C. Tanford, The Hydrophobic Effect: Formation of Micelles and Biological Membranes. 2nd ed. Wiley&Sons, New York, 1980.

43. J. A. Dean Dean, Lange's Handbook of Chemistry; McGraw Hill Book Company, New York, 1973, p. 5-5.

44. H. R. C. Ouiriques, M. F. S. Trinidade, M. C. Conceicao, S. Prasad, P. F. A. Filho, A. G. Souza, J. Therm. Calorimetry 75 (2004) 569.

45. M. Vinceković, Nano- and microcomplexes of biopolymer carrageenans and surfactants, PHD Thesis, Faculty of Science, University of Zagreb, 2009.

46. Y. Zheng, J. Liu, G. Ungar, P. V. Wright, Chem. Rec**.** 4 (2004) 176.

FIGURE CAPTIONS

Fig.1. FTIR spectra of DDACl, ιC and $(DDA)_2$ιC.

Figure 2. WAXD diffractograms of DDAκC (a), $(DDA)_2$ιC (b) , $(DDA)_3$λC (c) and DDACl (d).

Figure 3. TGA (top) and DTG (bottom) curves of (a) DDACl, (b) κC (dashed line) and DDAκC (full line), (c) ιC (dashed line) and $(DDA)_2$ιC (full line), and (d) λC (dashed line) and $(DDA)_3$λC (full line).

Fig. 4. DSC curves of the parent carrageenans (κC, ιC and λC) and DDACl (inset: T_{LC} is liquid crystallization temperature, T_i is isotropization temperature) on the first heating scan. κC – solid line; ιC –dashed line; λC – dotted line; T_g is glass transition temperature.

Fig. 5. First heating DSC curves of $(DDA)_n$CAR. DDAκC – dotted line; $(DDA)_2$ιC – solid line; $(DDA)_3$ λC – dashed line. T_g – glass transition temperature.

Fig. 6. Temperature dependence of SAXS patterns of DDAκC during heating from R.T. to 170 °C (bottom half) and during cooling from 170 °C to 50 °C (top half). Between the heating and cooling ramps, the sample was briefly heated to 210 °C. The successive curves are shifted vertically for clarity.

Fig. 7. Model of DDAκC in the layered LC state after a short annealing dynamics simulation: carbon (dark gray), hydrogen (light gray), oxygen (red), sulphate (yellow), nitrogen (blue).

Graphical Abstract

Model of dodecylammonium carrageenate in the layered liquid crystalline state after a short annealing dynamics simulation: carbon (dark gray), hydrogen (light gray), oxygen (red), sulphate (yellow), nitrogen (blue).